Biexciton emission from sol-gel ZnMgO nanopowders

C. H. Chia, Y. J. Lai, W. L. Hsu, T. C. Han, J. W. Chiou, Y. M. Hu, Y. C. Lin, W. C. Fan, and W. C. Chou

Articles you may be interested in

Structural, optical, vibrational, and magnetic properties of sol-gel derived Ni doped ZnO nanoparticles
J. Appl. Phys. **114**, 033912 (2013); 10.1063/1.4813868

Surface related and intrinsic exciton recombination dynamics in ZnO nanoparticles synthesized by a sol-gel method
Appl. Phys. Lett. **102**, 013109 (2013); 10.1063/1.4774002

High-excitation effect on photoluminescence of sol-gel ZnO nanopowder
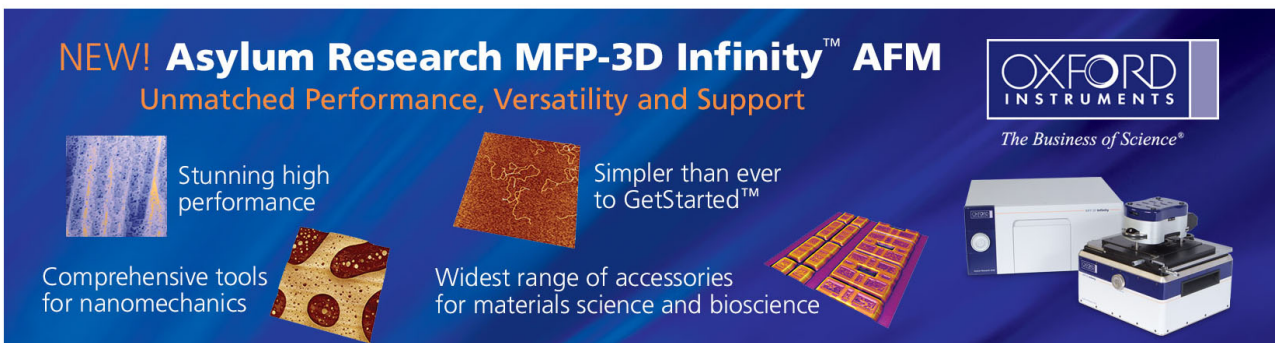Appl. Phys. Lett. **96**, 081903 (2010); 10.1063/1.3327338

Sol-gel synthesis and nonlinear optical transmission in Zn (1 x) Mg (x) O (x 0.2) thin films
Appl. Phys. Lett. **89**, 063102 (2006); 10.1063/1.2335375

Confinement-enhanced biexciton binding energy in ZnO/ZnMgO multiple quantum wells
Appl. Phys. Lett. **82**, 1848 (2003); 10.1063/1.1561158

Biexciton emission from sol-gel ZnMgO nanopowders

C. H. Chia,[1,a)] Y. J. Lai,[1] W. L. Hsu,[1] T. C. Han,[1] J. W. Chiou,[1] Y. M. Hu,[1] Y. C. Lin,[2] W. C. Fan,[2] and W. C. Chou[2]
[1]*Department of Applied Physics, National University of Kaohsiung, Kaohsiung 81148, Taiwan*
[2]*Department of Electrophysics, National Chiao Tung University, Hsin-Chu 30010, Taiwan*

We studied the power-dependent photoluminescence of $Zn_{1-x}Mg_xO$ nanopowders grown by sol-gel method, at temperature $T=100$ K. At moderate optical pumping intensity, a nonlinear emission band due to the radiative recombination of free biexcitons was detected. We found that the free biexciton binding energies of $Zn_{1-x}Mg_xO$ nanopowder ($0.01 \leq x \leq 0.05$) are nearly constant (13.5 ± 1.5 meV). © *2010 American Institute of Physics*. [doi:10.1063/1.3428780]

Excitonic optical properties of wide-gap semiconductors have intensively been studied to date from the point of view of both basic physics and device applications. It is expected that the contribution of excitonic processes to optical transitions in real device structures improves the performance of semiconductor optoelectronic devices. Therefore, it is important to study recombination dynamics of dense excitonic systems in wide-gap semiconductors from the point of view of exciton engineering. It is well established that the interaction between two excitons will lead to the formation of biexctions. The excitonic molecules will cause the emergence of nonlinear emission lines at the low-energy side of excitonic emission spectra.[1–5]

$Zn_{1-x}Mg_xO$ ternary alloy semiconductors are used as barrier layers for carrier confinement in highly efficient ZnO-based visible to near-UV quantum-well light-emitting devices.[3,6–9] There is also a large potential for the development of light-emitting devices operating in the UV-to-deep-UV spectral range using $Zn_{1-x}Mg_xO$ ternary alloy semiconductors as an active layer in quantum-well structures.[10–12] In ZnO quantum-well, the binding energy of biexcitons enhance significantly. In particular, the biexciton binding energy in ZnO quantum-well can be comparable to thermal energy of room-temperature (RT), indicating the possibility of biexciton lasing even at RT.[13–15] Therefore, study of photoluminescence (PL) of highly excited $Zn_{1-x}Mg_xO$ is important. In this letter, we report the luminescence from sol-gel $Zn_{1-x}Mg_xO$ nanopowders ($0.01 \leq x \leq 0.05$), taken at temperature $T=100$ K. At moderate optical pumping intensity, a nonlinear emission band due to the radiative recombination of free biexcitons was found. We estimated the biexciton binding energies of the $Zn_{1-x}Mg_xO$ ternary alloys by means of PL spectroscopy.

The $Zn_{1-x}Mg_xO$ nanopowders were grown from aqueous solution prepared using zinc nitrate hexahydrate [$Zn(NO_3)_2 \cdot 6H_2O$] and magnesium nitrate hexahydrate [$Mg(NO_3)_2 \cdot 6H_2O$] as the starting materials, de-ionized water as the solvent, and citric acid ($C_6H_8O_7$) as the stabilizer. The precursor solution was mixed thoroughly with a magnetic stirrer in 80 °C water bath until the formation of a sol. The sol was preheated in a furnace at 120 °C for 12 h to evaporate the solvent and remove the organic residuals. The

powders obtained from the dried sol were then annealed at 800 °C for 2 h at ambient air. We prepared three samples of $Zn_{1-x}Mg_xO$ ($x=0.01$, 0.03, and 0.05). The Mg concentration x in the samples were determined by energy dispersive x-ray spectroscopy with accuracy of 0.01. From the results of x-ray diffraction measurement (x-ray beam Cu $K_\alpha=0.154$ nm), no signal of MgO phase was detected from the samples. The crystalline size of the $Zn_{1-x}Mg_xO$ nanopowders was estimated to be about 50 nm by Sherrer's equation. Therefore, quantum confinement effect of excitons is not expected in the samples.

The PL spectra were measured by a 32-cm-long monochromator and a charge-coupled device camera. The samples were excited by 266 nm line of neodymium-doped yttrium aluminum garnet (Nd:YAG) laser for the low-T PL spectra. The pulsed laser has a pulse width of 10 ns and a repetition rate of 20 Hz. The excitation-power (I_{EXC}) dependence of the PL spectra was measured by using the 355 nm line of Nd:YAG laser and a variable neutral-density filter. A closed cycle refrigerator was used to perform the T-dependent measurement.

Figure 1(a) shows the low-T PL spectra of $Zn_{1-x}Mg_xO$ nanopowders, excited at low-I_{EXC} (~ 10 W/cm^2). As expected, the increase in Mg concentration x induces the blue-shift of excitonic PL bands.[10,11,16] Figure 1(b) shows the T-dependent PL peak energies for the $Zn_{1-x}Mg_xO$ nanopow-
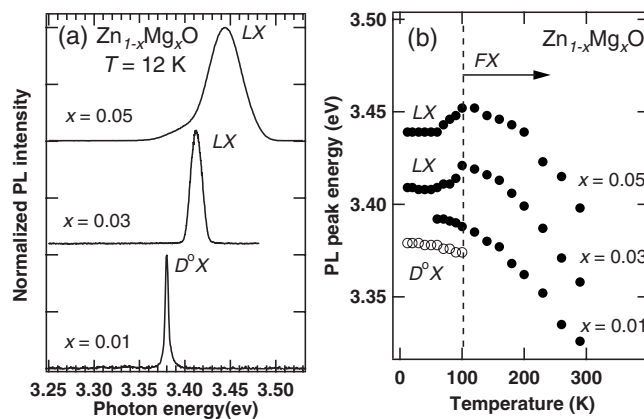

FIG. 1. (a) Low-T PL spectra of $Zn_{1-x}Mg_xO$ nanopowders taken at $T=12$ K. *LX*: localized exciton and D^oX: donor-bound exciton (b) T-dependent PL peak energies in $Zn_{1-x}Mg_xO$ nanopowders. The dashed line shows the T where the recombination of free excitons starts to dominate the luminescence.

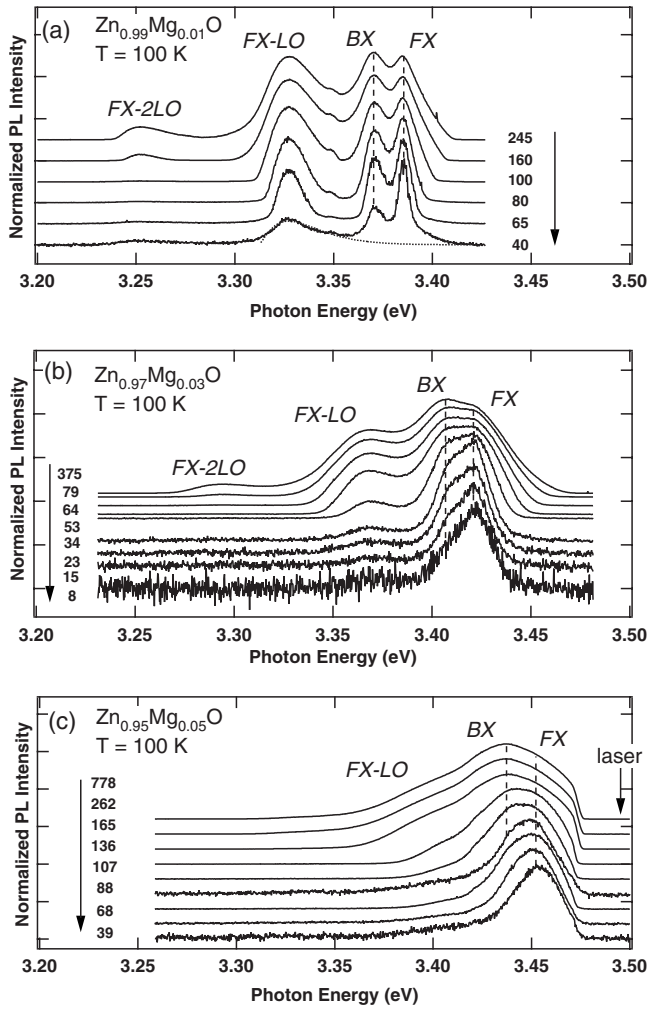a)Author to whom the correspondence should be addressed. Electronic mail: chchia@nuk.edu.tw.

FIG. 2. (a) Evolution of PL spectra as a function of I_{EXC} for $Zn_{1-x}Mg_xO$ nanopowders ($x=0.01$), taken at 100 K. The dotted line represents the fitting curve to *FX-LO* emission band, excited at $I_{EXC}=40$ W/cm^2. The dashed lines represent both the peak positions of free excitonic (*FX*) and free biexcitonic (*BX*) PL bands. (b) Evolution of PL spectra as a function of I_{EXC} for $Zn_{1-x}Mg_xO$ nanopowders ($x=0.03$), taken at 100 K. (c) Evolution of PL spectra as a function of I_{EXC} for $Zn_{1-x}Mg_xO$ nanopowders ($x=0.05$), taken at 100 K. The corresponding I_{EXC} for each spectrum are listed beside the spectra.

ders. At $x=0.03$ and 0.05, S-shaped dependence of PL peak energies were found, which is a unique feature originated from the thermal effect on radiative recombination of localized exciton (*LX*), due to alloy-fluctuation.[16] However, in the sample with $x=0.01$, this peculiar shift in PL peak energies is not observed, whereas a new emission line attributable to free exciton (*FX*) appears as *T* increases. Therefore, we assign the low-*T* PL band to the radiative recombination of donor-bound exciton (D^oX) (Ref. 17) for $Zn_{1-x}Mg_xO$ with $x=0.01$ and to the radiative recombination of *LX* for $Zn_{1-x}Mg_xO$ with $x=0.03$ and 0.05. From Fig. 1(b), notably, we can observe monotonic redshifts in the PL peak energies, indicating the *FX* recombination dominates the PL spectra after $T=100$ K.

We measured the I_{EXC}-dependence of PL spectra at $T=100$ K. The highly excited PL of the $Zn_{1-x}Mg_xO$ nanopowders with $x=0.01$, 0.03, and 0.05, were shown in Figs. 2(a)–2(c), respectively. All of the spectra were normalized with the peak intensities of the corresponding *FX* emission lines. The I_{EXC}'s for each spectrum are shown beside the

spectra (in units of W/cm^2). In Figs. 2(a)–2(c), except the two main emission lines (denoted as *FX* and *BX*), there are two emission bands (denoted as *FX-LO* and *FX-2LO*) at the low-energy range of the spectra. In Fig. 2(a), we fitted the *FX-LO* emission line of the $Zn_{0.09}Mg_{0.01}O$ alloy ($I_{EXC}=40$ W/cm^2), by the expression $I_{LO} \propto (\hbar\omega - E_{FX} - E_{LO})^{1.5} \exp[-(\hbar\omega - E_{FX} - E_{LO})/k_B T_e]$, which describes the PL line shape of longitudinal phonon (*LO*)-assisted recombination of excitons.[4,18] The fitting curve (dotted line) matches well the emission band, with parameters; free exciton energy E_{FX} (3.385 eV), *LO*-phonon energy E_{LO} (73 meV)[19] and lattice temperature T_e (119 K). Therefore, it is reasonable to assign the PL band to *LO*-phonon sideband of *FX*. Also, a small hump located at low-energy side of the *FX-LO* emission line is the 2*LO*-phonon sideband of *FX* because the spectral separation between them is 73 meV.

In Fig. 2(a), the emission band with peak energy 3.385 eV is due to radiative recombination of *FX*. The PL band (denoted as *BX*) is attributable to the radiative recombination of free biexciton (*BX*), based on the following reasons. (i) As I_{EXC} increases, the *BX* line grows superlinearly against the *FX* line, and its peak intensity exceeds that of the *FX* line at high-I_{EXC}. (ii) It is well known that the spectral shape of *BX* emission could be expressed by an inverse Boltzmann distribution function,[4] which exhibits an asymmetric emission band with significant low-energy tail. As I_{EXC} increases, we note that the *BX*-emission line shape is more asymmetric at low-energy. (iii) Furthermore, an annihilation of biexciton with kinetic energy $\hbar^2 k^2/4M_{EX}$, leaving a photon ($k \sim 0$) and an exciton with kinetic energy $\hbar^2 k^2/2M_{EX}$, yields the biexcitonic transition energy $E_{BX} = E_{FX} - E_{BX}^b - \hbar^2 k^2/4M_{EX}$,[20,21] with E_{BX}^b and M_{EX} being the free biexciton binding energy and the exciton effective mass. Neglecting the kinetic energy term $\hbar^2 k^2/4M_{EX}$, the E_{BX} can be obtained from the difference between E_{FX} and E_{BX}^b. We can expect a comparable E_{BX}^b of ZnMgO alloy to that of ZnO because the binding potential of electron-hole pairs in ZnMgO is close to that in ZnO.[22,23] The peak energy of the *BX* line from the $Zn_{1-x}Mg_xO$ nanopowders ($x=0.01$) is 3.370 eV, as shown in Fig. 2(a). This yields an energetic difference of 15 meV with the peak energy of the *FX* line. This value is close to the E_{BX}^b of ZnO.[4] On the basis of the abovementioned findings, we believe that the *BX* emission band could be attributed to the radiative recombination of free biexcitons.

In the case of the $Zn_{1-x}Mg_xO$ nanopowders ($x=0.03$ and 0.05), the I_{EXC}-dependent PL spectra are shown in Figs. 2(b) and 2(c), respectively. The *BX* emission bands also emerge as I_{EXC} increases and have the following characteristics: (i) superlinear growth of emission intensity against the *FX* emission line, (ii) asymmetric line shape at low-energy side, and (iii) comparable E_{BX}^b with ZnO. In Fig. 2(c), an anomaly in the PL line shape at about 3.47 eV is not intrinsic but due to the cutting edge of the long-wave pass filter (eliminating the 3.493 eV-laser line), used in the measurement. The peak positions of the *BX* emission bands are 3.407 and 3.437 eV for the $Zn_{1-x}Mg_xO$ nanopowders with $x=0.03$ and 0.05, respectively. Also, the peak positions of the *FX* emission bands are 3.421 and 3.452 eV for the $Zn_{1-x}Mg_xO$ nanopowders with $x=0.03$ and 0.05, respectively. Therefore, we can obtain the E_{BX}^b's are about 15 meV for both samples.

Figure 3 shows the *T*-dependent PL of $Zn_{0.97}Mg_{0.03}O$ nanopowder ($I_{EXC}=375$ W/cm^2). As *T* increases, all of the
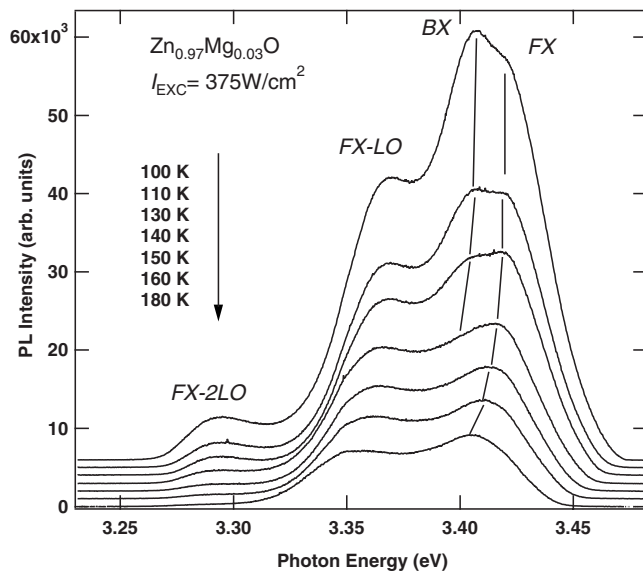
FIG. 3. *T*-dependent PL spectra of $Zn_{1-x}Mg_xO$ nanopowders ($x=0.03$) under $I_{EXC}=375$ W/cm^2. The solid lines label the shifts in *FX* and *BX* emission peak energies. The *BX* emission completely disappears at $T=140$ K.

emission band redshift. We can observe the intensity of the *BX* transition gradually decreases, and finally diminishes between $T=130$ and 140 K, of which the thermal energy is equal to 12 meV. The complete disappearances of *BX* emission line between $T=130$ and 140 K were also found in the $Zn_{1-x}Mg_xO$ nanopowders with $x=0.01$ and 0.05. The value 12 meV is slightly smaller than the E_{BX}^b determined above. Indeed, the E_{BX}^b determined from the difference between E_{BX} and E_{FX} should be the upper bound value for E_{BX}^b because of the thermal distribution of *FX* and *BX* at $T=100$ K. Therefore, it is believed that a more realistic E_{BX}^b of the $Zn_{1-x}Mg_xO$ nanopowder ($0.01 \leq x \leq 0.05$) should lie between 12 and 15 meV (or 13.5 meV $\pm$ 1.5 meV).

In conclusion, we observed the emissions from biexcitonic transitions in the $Zn_{1-x}Mg_xO$ nanopowder with $0.01 \leq x \leq 0.05$, grown by sol-gel method. The free biexciton binding energies of the ZnMgO alloys were determined by PL spectroscopy. It was found that the free biexciton binding energies are nearly constant at 13.5 ± 1.5 meV, as the Mg concentration *x* increases from 0.01 to 0.05.

[1] H. J. Ko, Y. F. Chen, T. Yao, K. Miyajima, A. Yamamoto, and T. Goto, Appl. Phys. Lett. **77**, 537 (2000).
[2] C. J. Pan, K. F. Lin, and W. F. Hsieh, Appl. Phys. Lett. **91**, 111907 (2007).
[3] H. D. Sun, T. Makino, Y. Segawa, M. Kawasaki, A. Ohtomo, K. Tamura, and H. Koinuma, Appl. Phys. Lett. **78**, 3385 (2001).
[4] A. Yamamoto, K. Miyajima, T. Goto, H. J. Ko, and T. Yao, J. Appl. Phys. **90**, 4973 (2001).
[5] F. Y. Jen, Y. C. Lu, C. Y. Chen, H. C. Wang, C. C. Yang, B. P. Zhang, and Y. Segawa, Appl. Phys. Lett. **87**, 072103 (2005).
[6] M. Zamfirescu, A. Kavokin, B. Gil, G. Malpuech, and M. Kaliteevski, Phys. Rev. B **65**, 161205 (2002).
[7] C. Morhain, T. Bretagnon, P. Lefebvre, X. Tang, P. Valvin, T. Guillet, B. Gil, T. Taliercio, M. Teisseire-Doninelli, B. Vinter, and C. Deparis, Phys. Rev. B **72**, 241305 (2005).
[8] B. Gil, P. Lefebvre, T. Bretagnon, T. Guillet, J. A. Sans, T. Taliercio, and C. Morhain, Phys. Rev. B **74**, 153302 (2006).
[9] T. Bretagnon, P. Lefebvre, T. Guillet, T. Taliercio, B. Gil, and C. Morhain, Appl. Phys. Lett. **90**, 201912 (2007).
[10] H. Shibata, H. Tampo, K. Matsubara, A. Yamada, K. Sakurai, S. Ishizuka, S. Niki, and M. Sakai, Appl. Phys. Lett. **90**, 124104 (2007).
[11] H. Tampo, H. Shibata, K. Maejima, A. Yamada, K. Matsubara, P. Fons, S. Niki, T. Tainaka, Y. Chiba, and H. Kanie, Appl. Phys. Lett. **91**, 261907 (2007).
[12] H. Zhu, C. X. Shan, B. H. Li, Z. Z. Zhang, J. Y. Zhang, B. Yao, D. Z. Shen, and X. W. Fan, J. Appl. Phys. **105**, 103508 (2009).
[13] H. D. Sun, T. Makino, N. T. Tuan, Y. Segawa, Z. K. Tang, G. K. L. Wong, M. Kawasaki, A. Ohtomo, K. Tamura, and H. Koinuma, Appl. Phys. Lett. **77**, 4250 (2000).
[14] C. H. Chia, T. Makino, K. Tamura, Y. Segawa, M. Kawasaki, A. Ohtomo, and H. Koinuma, Appl. Phys. Lett. **82**, 1848 (2003).
[15] J. A. Davis, L. V. Dao, X. Wen, P. Hannaford, V. A. Coleman, H. H. Tan, C. Jagadish, K. Koike, S. Sasa, M. Inoue, and M. Yano, Appl. Phys. Lett. **89**, 182109 (2006).
[16] T. A. Wassner, B. Laumer, S. Maier, A. Laufer, B. K. Meyer, M. Stutzmann, and M. Eickhoff, J. Appl. Phys. **105**, 023505 (2009).
[17] M. Grundmann and C. P. Dietrich, J. Appl. Phys. **106**, 123521 (2009).
[18] C. Klingshirn, Phys. Status Solidi B **71**, 547 (1975).
[19] Ü. Özgür, Y. I. Alivov, C. Liu, A. Teke, M. A. Reshchikov, S. Doğan, A. Avrutin, S.-J. Cho, and H. Morkoc, J. Appl. Phys. **98**, 041301 (2005).
[20] C. Klingshirn and H. Haug, Phys. Rep. **70**, 315 (1981).
[21] H. Souma, T. Goto, T. Ohta, and M. Ueta, J. Phys. Soc. Jpn. **29**, 697 (1970).
[22] R. Schmidt, B. Rheinländer, M. Schubert, D. Spemann, T. Butz, J. Lenzner, E. M. Kaidashev, M. Lorenz, A. Rahm, H. C. Semmelhack, and M. Grundmann, Appl. Phys. Lett. **82**, 2260 (2003).
[23] J. G. Lu, Y. Z. Zhang, Z. Z. Ye, Y. J. Zeng, J. Y. Huang, and L. Wang, Appl. Phys. Lett. **91**, 193108 (2007).